Int. J. Heat Mass Transfer. Vol. 15, pp. 247–260. Pergamon Press 1972. Printed in Great Britain

HEAT TRANSFER AND FLOW RESISTANCE IN CONDENSATION OF LOW PRESSURE STEAM FLOWING THROUGH TUBE BANKS

T. FUJII, H. UEHARA, K. HIRATA and K. ODA

Research Institute of Industrial Science, Kyūshū University, Fukuoka, Japan

(*Received* 22 *June* 1970)

Abstract—This paper deals with an experiment performed on condensation, when saturated steam of low pressure flows through tube banks, crossing them horizontally. Simple expressions for heat transfer coefficients of steam side and pressure drops through tube banks are proposed, and resistance coefficients are represented graphically. At the same time, a comparison is made between the results for the two tube banks of in-line and staggered arrangement with 22/14 spacing-to-diameter ratio. Such results of observation as peripheral distribution of temperature on tube surface, accumulation of leaked air, breathing flow of steam etc. are also reported.

NOMENCLATURE

c_D, resistance coefficient defined by (7) or (8);

c_p, specific heat at constant pressure [J/kg deg];

D, outer diameter of a tube [m];

Fr, Froude number $= M^2/\bar{\rho}gD$;

G, condensation rate per tube row per unit maximum flow area [kg/m² s];

Gr, Grashof number $= \rho^2 gD^3/\mu^2$;

g, gravitational acceleration [m/s²];

H, nondimensional number of condensation $= c_p(T_s - T_w)/PrL$;

L, latent heat of condensation [J/kg];

M, mass velocity of steam through maximum flow area [kg/m² s];

N, necessary number of tube rows for complete condensation defined by (12);

Nu, Nusselt number defined by (2);

n, number of tube rows contained in a control surface;

p, pressure of steam [bar];

Pr, Prandtl number;

q, average heat flux for a tube row [W/m²];

R, $\rho\mu$-ratio $= (\rho\mu/\bar{\rho}\bar{\mu})^{\frac{1}{2}}$;

Re, Reynolds number for maximum flow area $= \rho MD/\bar{\rho}\mu$;

$\overline{Re}_\xi$, Reynolds number for minimum flow area $= \zeta MD/\bar{\mu}$;

T_s, temperature of steam [°C];

$T_{w\theta}$, temperature of outer tube surface [°C];

T_w, average temperature of outer tube surface [°C].

Greek symbols

α, heat-transfer coefficient of steam side, defined by (1) [W/m² deg];

ζ, ratio of maximum flow area to minimum one;

θ, angle measured clockwisely from leading stagnation of a tube [deg];

λ, thermal conductivity [W/m² deg];

μ, dynamic viscosity [kg/ms];

ξ, ratio of mean square mass velocity to M^2;

ρ, density [kg/m³];

φ, χ, ψ, nondimensional parameters defined by (3), (5) and (4) respectively.

Subscripts

i, j, N, i-, j- and N-th cross section from the inlet of tube bank, i.e. the cross sections of maximum flow area just below i-, j- and N-th tube row respectively;

m, arithmetic mean value of i and j;

0, inlet of tube bank.

Superscripted properties with $^{-}$ for steam, and unsuperscripted properties for condensate. All physical properties are evaluated at the saturation temperature of steam.

1. INTRODUCTION

IN KEEPING step with ever-increasing size of steam turbine units, the design of condensers has been improved. The most efficient arrangement of tubes or tube banks in the condenser, however, has not been established. In this problem, it is most fundamental to predict the variation of both condensation heat transfer and pressure of low pressure steam through tube banks. Nevertheless there is little experimental information available on pressure drops.

This paper presents some experimental results on condensation of saturated steam which was obtained by using two tube banks of in-line and staggered arrangement of 22/14 spacing-to-diameter ratio. The tests are performed in the ranges of steam pressure 0·01–0·07 bar, oncoming velocities of steam 10–40 m/s and temperatures of cooling water 5–20°C. Incidentally, other problems clarified here involve peripheral distribution of temperature on tube surface, leaving behavior of condensate from tubes, accumulation of leaked air, and breathing flow of steam. These will provide some necessary conditions to be considered in theoretical treatment of condensation heat transfer.

2. APPARATUS

Figure 1 shows a closed natural circulation loop of steam and the condensate, which could be air-tightened up to a limit of about 10 lussec, that is, the pressure rise rate about 10^{-8} bar/s. The whole loop is thermally insulated by asbestos and woolly-felt of 10–30 mm thickness. The flow rate and pressure of steam are regulated by the electric imput to boiler and by the flow rates of cooling water to the test tube bank and subsidiary condenser.

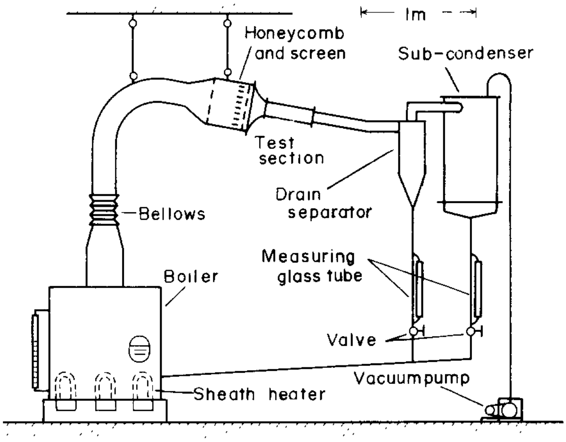

FIG. 1. A circulation loop of steam and the condensate.

Figure 2 shows two tube banks used for the in-line and staggered arrangement. Each bank is composed of brass tubes of 14·0 mm o.d., 10·4 mm i.d. and 100 mm heat-transferring length, which are arranged in 15 rows by 22 mm spacing both to the direction of steam flow and at right angles with it. The tube bank is settled in the test section so that the tubes may be horizontal and the steam may flow slightly downward from horizontal in an angle of about ten degrees. The tubes in each row are connected in succession outside the tube bank, and cooling water flows into the lowest tube, leaving the highest tube.

In the middle tubes of every row composed of five tubes and in the second tubes from the top of every row composed of four tubes, four holes of 1 mm dia. and 25 mm effective depth are drilled at peripherally equal intervals, namely, at the leading and trailing stagnation and at right angles with them. A copper–constantan thermocouple of 0·3 mm dia. is

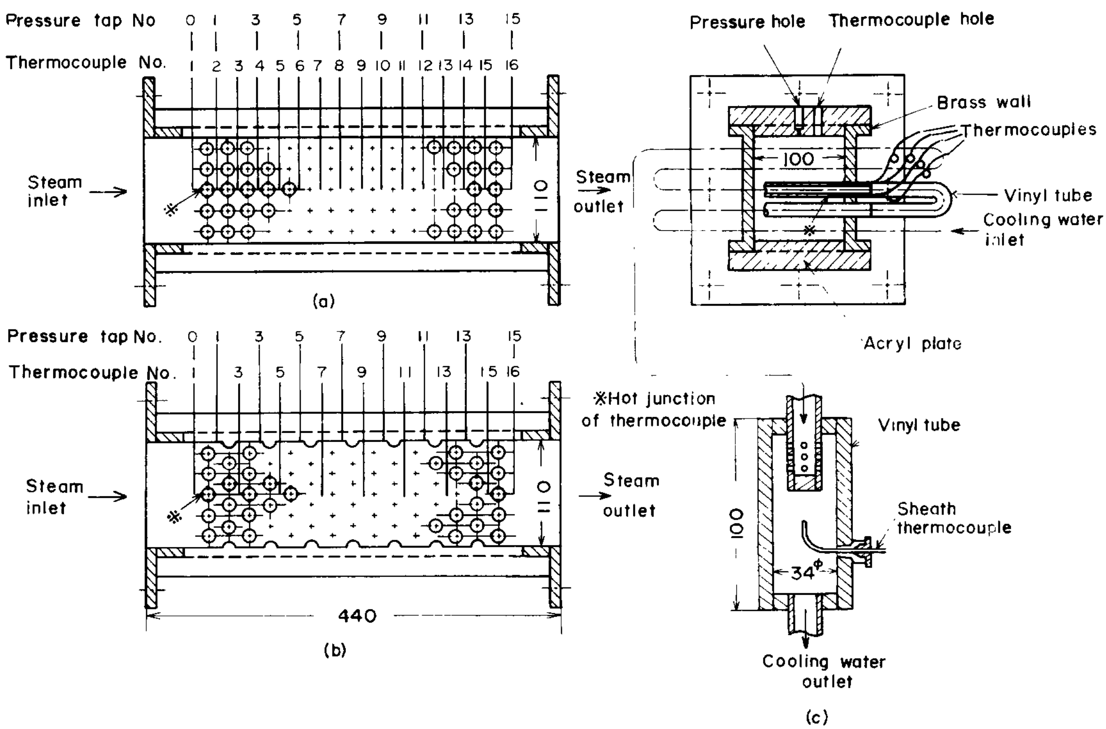

FIG. 2. Tube banks.
(a) in-line arrangement, (b) staggered arrangement, (c) mixing chamber of cooling water.

inserted into each hole. If the hot junction is assumed to be set in the middle of the tube thickness only, the surface temperature can be exterpolated by using the equation of thermal conduction. Preliminarily, it was confirmed that the axial gradient of the surface temperature of the tubes is much smaller than that of the temperature of the cooling water. Steam temperature and bulk mean temperature of cooling water entering and leaving the tubes are measured by copper–constantan sheath thermocouples of 1·6 mm dia. The electro-motive forces of the thermocouples were normally printed on strip charts of four sets of self-balancing electronic recorder of 24 point self-switching and 2·5 mV full scale, and especially in the case of small and fluctuating temperature difference, they were continuously recorded by a two-pen recorder of 0·1–1 mV full scale.

For measuring taps of steam pressure, there were drilled nine holes of 3·2 mm dia. on the top cover of the tube banks at the positions as shown in Fig. 2 and those of 2 mm diameter on another tube bank of staggered arrangement. The pressure at No. 15 tap was taken as a standard one and measured by a Göttingen type mercury manometer. The differences between the pressure at each tap and this standard pressure were measured by a U-tube "Bizen" manometer.

The flow rate of cooling water through each tube row was measured by 15 sets of an inverse U-tube water manometer and an orifice, and was distributed uniformly within the accuracy of 2 per cent. The total condensation rate of the tube bank was evaluated with accumulation rate of the condensate in both a pipe led from a drain separator and a measuring glass tube, where the flow of the condensate was shut off by the valve shown in Fig. 1.

The electric input to boiler and the total rate of condensation were in good agreement within the accuracy of measurement, but the sum of the heat rates given to cooling water was usually a few per cent, sometimes about 10 per cent higher than the total rate of condensation. It seems that the cooling water was over-heated by surrounding air for the most part and by the side walls of the tube bank partly. The heat rate for each tube row, therefore, was corrected on the basis of the total rate of condensation and in proportion to the temperature rise of cooling water.

3. RESULTS AND CONSIDERATIONS

When the measurement of heat-transfer coefficients was attempted, the temperature of saturated steam was kept higher than room temperature by one or two degrees, lest the steam should be super-heated. When the measurement of pressure drops was attempted, on the other hand, steam temperature was kept lower than room temperature by one or two degrees, lest the lead pipings to manometers should be blocked by drain. It was impossible, therefore, to take these two kinds of data simultaneously.

Dropwise condensation took place only on the fresh surface of tubes for the runs of the first experimental day. For the runs after the second day continued at some intervals, filmwise condensation became dominant on all tube surfaces. The cause seems due to the change of microscopic state of the tube surface. The ranges of data on heat transfer are shown in Table 1, in which Run Nos. 8–11 correspond to dropwise condensation and the other to filmwise.

3.1 *Observations*

Figure 3 shows an example of measurements of steam temperature T_s, average temperature of outer tube surface T_w, heat flux q, heat-transfer coefficient α and steam velocity $M/\bar{\rho}$ for in-line arrangement corresponding to Run No. 1 in Table 1. Steam has condensed almost completely on its passage to 9th row. Steam temperature falls more rapidly over subsequent rows, where leaked air was accumulated. That tendency was

Table 1. Measurements for heat transfer coefficients

Run	Symbol	Steam M_0	M_{15}	T_{s0}	T_{s15}	Cooling water w	T_{in}	T_{out}	T_w	$M' \times 10^3$	M''/M'
1		0·380	0	34·29	10·86	0·490	7·65	13·94	31·79	4·18	1·08
2	○	0·466	0	29·86	13·77	0·550	5·07	10·54	27·42	5·13	1·05
3	□	0·647	0	34·48	34·11	0·505	7·75	14·16	32·39	7·12	0·97
4	△	0·845	0	35·33	34·76	0·740	8·27	13·60	33·13	9·02	1·01
5	◇	0·892	0	33·86	33·63	0·855	7·30	12·63	30·42	9·81	1·00
6	▽	1·278	0	37·55	37·16	1·350	10·72	15·44	34·09	14·05	1·02
7	◭	1·236	0·257	37·02	36·80	1·215	15·50	19·65	34·02	13·60	1·06
8	Y	0·394	0	33·59	11·27	0·825	8·27	13·47	31·33	4·67	1·02
9	×	0·623	0	33·62	13·92	0·825	7·03	12·49	31·26	6·85	1·04
10	+	0·868	0	34·36	29·36	0·825	7·11	12·90	31·79	9·33	1·08
11	*	1·271	0·132	38·19	37·54	0·925	10·57	16·53	35·55	13·98	0·97
12	◆	0·417	0	26·22	26·01	0·634	7·70	11·36	24·93	4·59	1·06
13	■	0·631	0	27·76	22·51	1·100	7·73	11·13	25·83	6·93	1·11
14	▲	0·817	0	31·90	31·22	1·186	8·01	11·91	29·36	10·10	1·07

Run No. 1–7, filmwise, in-line; No. 8–11, dropwise, in-line; No. 12–14, filmwise, staggered. M_0 (kg/m^{2}s), mass velocity of steam at the inlet of tube bank; M_{15} (kg/m^2 s), mass velocity of steam at the outlet of tube bank; T_{s0} (°C), temperature of steam at the inlet of tube bank; T_{s15} (°C), temperature of steam at the outlet of tube bank; w (m/s), mean velocity of cooling water; T_{in} (°C), temperature of cooling water at the inlet of tubes; T_{out} (°C), temperature of cooling water at the outlet of the first tube row; T_w (°C), mean surface temperature of the first tube row; M' (kg/s), total condensation rate measured; M'' (kg/s), total condensation rate evaluated with the heat rate given to cooling water.

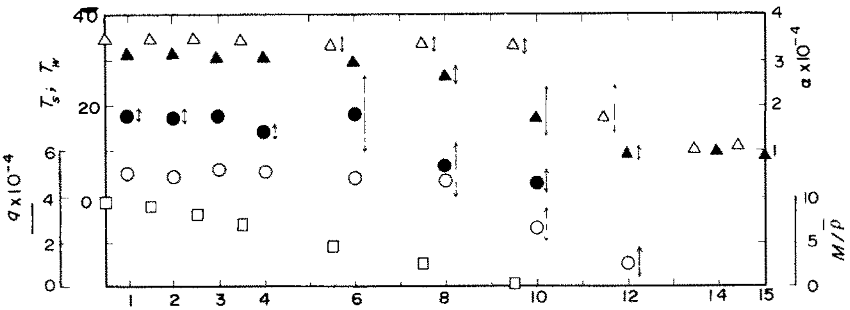

FIG. 3. Variations of steam temperature T_s (°C) (△), tube surface temperature T_w (°C) (▲), heat flux q(W/m^2) (○), heat transfer coefficient α (W/m^2 deg) (●) and steam velocity $M/\bar{\rho}$ (m/s) (□) across the tube bank for Run No. 1 in Table 1.

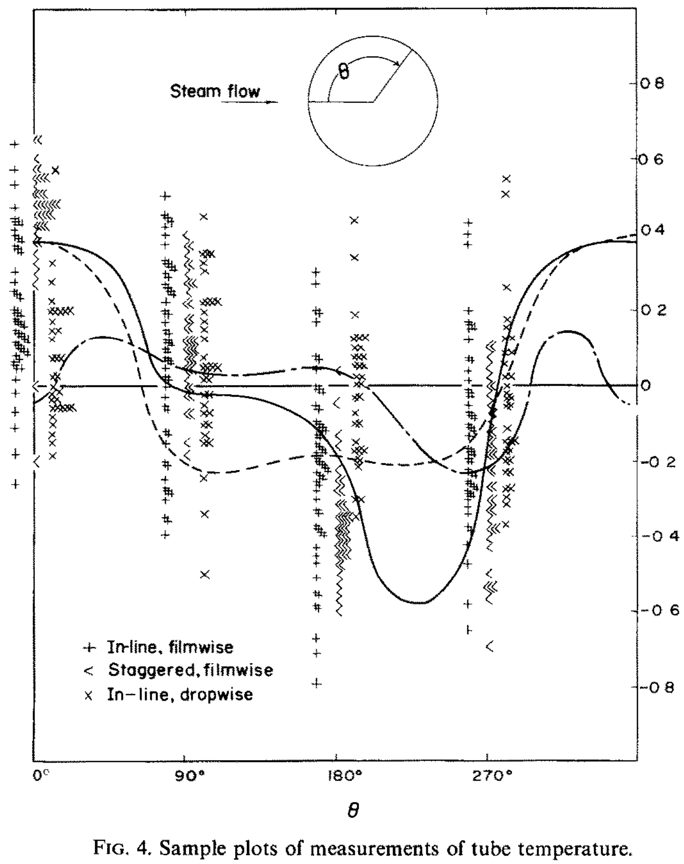

FIG. 4. Sample plots of measurements of tube temperature.

usual in the cases where mass flow rate of steam was relatively small.

Temperatures of steam, tube surface and cooling water leaving tubes and pressure of steam normally fluctuated with period of about 10–20 s. Some examples of their amplitude are also shown as vertical bars in Fig. 3. These fluctuations are remarkable on two or three tube rows corresponding to the boundary between steam flow zone and accumulated air zone, in both cases of dropwise and filmwise condensation. These phenomena may be ascribed to breathing flow of steam, which may be provoked by the swaying of the steam–air boundary, and which was also conceived occasionally by the appearance and disappearance of dew inside the top cover.

Figure 4 shows the sample plots of measurements of tube surface temperature nondimensionalized by $(T_s - T_w)$. There are cases when the difference between the maximum and minimum temperature on a tube is about 1·5 times as large as $(T_s - T_w)$ in that case. The distribution of $[1 - (T_{w\theta} - T_w)/(T_s - T_w)]$ in the figure suggests that of the film thickness of condensate. Three curves inserted in the figure are some of the results obtained preliminarily on a single tube [1]. At the same time, it was also confirmed that arithmetic mean of the readings of the electromotive force of four thermocouples inserted at peripherally equal intervals was in good agreement with that of eight thermocouples inserted similarly within the accuracy of about three per cent in $(T_s - T_w)$ on every pattern of temperature distribution. In this paper, the arithmetic mean of measurements at aforementioned four positions is adopted as the mean surface temperature, though the patterns of temperature distributions for in-line and staggered arrangement and in the cases of filmwise and dropwise condensation seem to be somewhat different from each other and also from those on a single tube.

For dropwise condensation as shown in Fig. 5(a), drops coalescent up to about 5 mm dia. on the tube surface were blown away into steam flow from any sites, consequently it seemed that the sweeping effect of the drops was not so widely extended as in the case hitherto stated for the experiments on a vertical plate in quiescent steam. For filmwise condensation as shown in Fig. 5(b), relatively large breast-like drops developed at certain two or three positions along the lowest line on the tube where steam velocity was low or along the trailing stagnation on the tube where steam velocity was high, then they drained off at a regular interval. By the way, a drop of the drain was estimated to be about 0·4 g in mass, which was about ten times as weighty as aforementioned drops with dropwise condensation. Where leaked air was accumulated, drops of relatively large but unequal size adhered at random to the tube surface, as shown in Fig. 5 (c), but they remained in size, without leaving the tube.

3.2 *Nondimensional correlations for steam side heat transfer*

Heat transfer coefficient on steam side α and Nusselt number Nu are defined respectively as,

$$\alpha = \frac{q}{(T_s - T_w)}, \tag{1}$$

$$Nu = \frac{\alpha D}{\lambda}, \tag{2}$$

where q is evaluated with the flow rate and temperature rise of cooling water, which is corrected in some cases by using total rate of condensation in proportion to the temperature rise of respective tubes, T_s is the reading of thermocouple settled just before each tube row or the value interpolated from the readings at just upstream and downstream for the tube row composed of four tubes, and T_w is peripheral mean surface temperature at about middle part of the row. The heat-transfer coefficient thus defined may be regarded as surface mean value for the tube row, because q scarcely varied along the tube axis in the case that the temperature rise of cooling water is much smaller

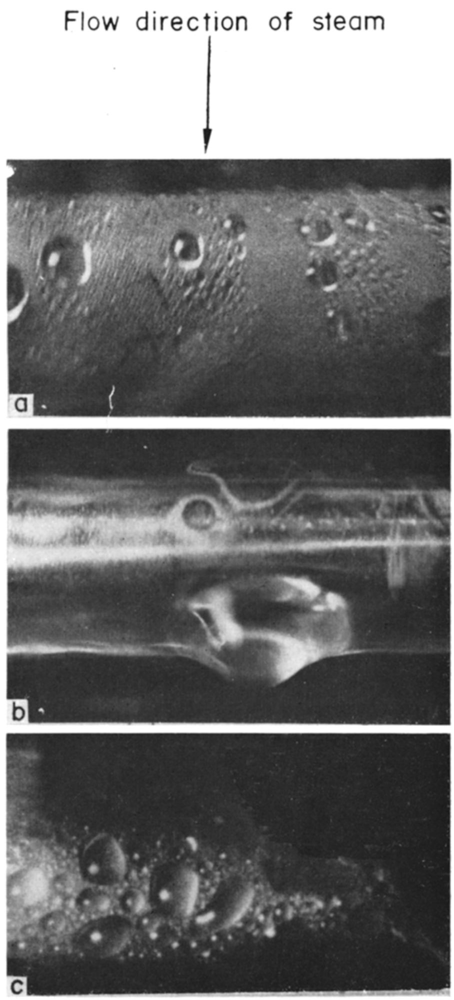

FIG. 5. Condensate on a tube.
(a) Dropwise condensation. Photo is taken from the upper side of in-link bank.
(b) A breast-like drop in filmwise condensation. Photo is taken from the lower side of staggered bank.
(c) Drops where leaked air is accumulated. Photo is taken from the upper side of staggered bank.

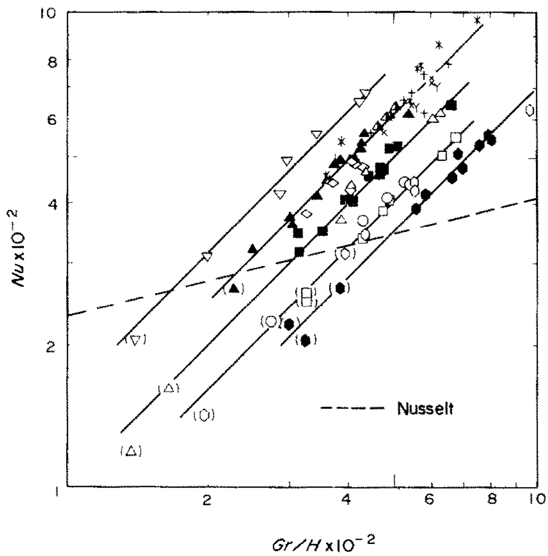

FIG. 6. Correlation between Nu and Gr/H. Symbols correspond to those in Table 1.

than the temperature difference between steam and cooling water.

Figure 6 shows the correlation between Nu and Gr/H. These two parameters lack general correspondence. The fact that they are proportional only under the same experimental run corresponds to the fact that heat fluxes are not different with every tube row. This is reasonable, because the thermal resistance inside tube is much larger than outside one. The dotted line inserted in the figure shows the value predicted by Nusselt's theory, which corresponds to the heat transfer from quiescent steam to a horizontal tube. The data plotted below this dotted line, as parenthesized also in Figs. 7 and 8, may be affected by the accumulated air, since they pertain to the tubes in the boundary zone of steam and air.

Figures 7 and 8 show the correlations between Nu and φ, Nu and ψ respectively, where

$$\varphi = \chi Re^{\frac{1}{2}}, \tag{3}$$

$$\psi = \chi \left(1 + \frac{0{\cdot}276}{\chi^4 FrH}\right)^{\frac{1}{4}} Re^{\frac{1}{2}}, \tag{4}$$

$$\chi = 0{\cdot}9\left(1 + \frac{1}{RH}\right)^{\frac{1}{3}}. \tag{5}$$

These parameters are derived by the authors [1] from the theory of filmwise condensation on a

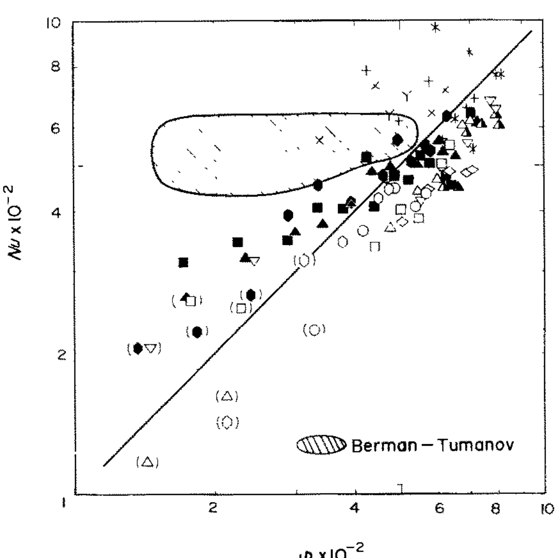

FIG. 7. Correlation between Nu and φ. Symbols correspond to those in Table 1.

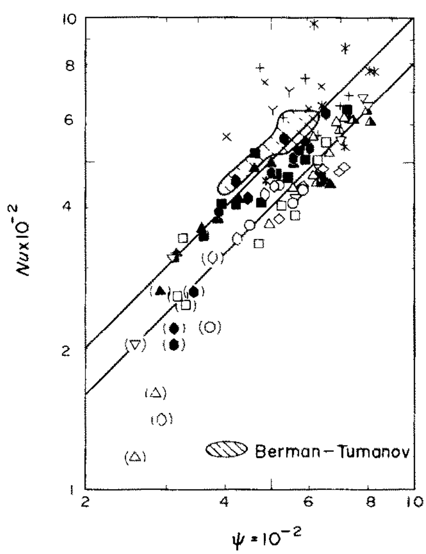

FIG. 8. Correlation between Nu and ψ. Symbols correspond to those in Table 1.

horizontal tube placed in the downward flow, and φ corresponds to forced convection only and ψ to combined convection of forced and body force.

The correlation for dropwise condensation in Figs. 7 and 8 is naturally no good and the heat-transfer coefficients are about $(2{\cdot}5\text{–}3{\cdot}5) \times 10^4$ (W/m^2 deg) for 0·053 bar and about $(3\text{–}4) \times 10^4$ (W/m^2 deg) for 0·067 bar. It is remarkable that these values are in good agreement with those obtained theoretically by Tanner *et al.* [2] and those obtained experimentally by Brown–Thomas [3] in quiescent steam of similarly low pressures. At low pressure, the heat transfer coefficient for dropwise condensation does not increase so much in comparison with that for filmwise condensation.

For filmwise condensation, the scattering of data in Fig. 7 is mainly due to the data on low steam velocity. Figure 8 shows that parameter ψ, which is derived theoretically under the assumption that the directions of both steam flow and gravity are parallel, is also applicable to the case where these directions are at right angles. The overall accuracy of these experiments may be estimated to be about ten per cent.

In Fig. 8 the data which are mixed together for in-line and staggered arrangement pertain to the tube rows from the inlet of each bank to the second or the third, and the correlation of the parenthesized data affected by the accumulated air are no good. On the whole, however, the Nusselt number for the case of staggered arrangement is in good agreement with the theoretical one for a single tube, and that for in-line is lower than this by about 20 per cent. This discrepancy may be ascribed to the difference of flow pattern around tubes. From Fig. 8 there may be proposed the following expression,

$$Nu = K\chi\left(1 + \frac{0{\cdot}276}{\chi^4 FrH}\right)^{\frac{1}{4}} Re^{\frac{1}{2}}, \tag{6}$$

where $K = 0{\cdot}8$ for in-line and $K = 1{\cdot}0$ for staggered.

The data of Berman–Tumanov of 129 points plotted in Fig. 4 of [4] have been rearranged by parameters φ and ψ, and are given in Figs. 7 and 8 as hatched areas. Their experiments were performed on a tube of 19 mm dia., the situation of which was resembled to the tubes in the second row of staggered tube bank in this paper, and the steam flowed vertically downwards and the velocity was extended to very low ranges. The correlation of their data in Fig. 8 has become very good, and expressed by (6) with $K = 1{\cdot}1 \pm 0{\cdot}1$. The cause that the coefficient K is somewhat larger due to the systematic error concerning measurements of surface temperature and heat flux.

Table 2. Experimental conditions for the measurements of pressure drop of condensing steam

Run	Symbol	$p_0 \times 10^3$ (bar)	M_0 (kg/m^2 s)	$G \times 10^3$ (kg/m^2 s)	N	$P_1 \times 10^3$ (bar)	$P_N \times 10^3$ (bar)	$(\overline{R_\zeta})_0 \times 10^3$
1	□	20·9	0·868	23·4	37	19·1	14·5	3·76
2	△	27·2	0·857	19·2	45	25·8	21·8	3·66
3	▽	27·2	0·661	25·8	26	26·4	25·3	2·81
4	○	13·8	0·441	11·9	37	13·1	11·6	1·94
5	⊓	44·5	1·19	25·6	47	43·4	33·5	4·98
6	[illegible]	40·5	0·881	31·1	28	39·8	36·5	3·70
7	[illegible]	29·3	0·409	11·9	34	29·1	27·7	1·73
8	■	26·1	0·874	23·2	38	26·0	17·3	3·71
9	▲	27·9	0·619	30·6	20	27·4	25·7	2·62
10	●	18·0	0·289	9·0	32	18·1	17·0	1·24

Run No. 1–4, in-line, pressure tap of 3·2 mm hole dia.; No. 5–7, staggered, pressure tap of 3.2 mm hole dia.; No. 8–10, staggered, pressure tap of 2·0 mm hole dia. N and p_1, p_N are evaluated with (12) and (11) respectively.

For the heat transfer concerning tube banks, Short–Brown [5], and Young–Wohlenberg [6] experimented with Freon vapour and Rachko [7] with steam. These data shows higher values than Nusselt prediction, but cannot be compared quantitatively because vapour velocity is not represented.

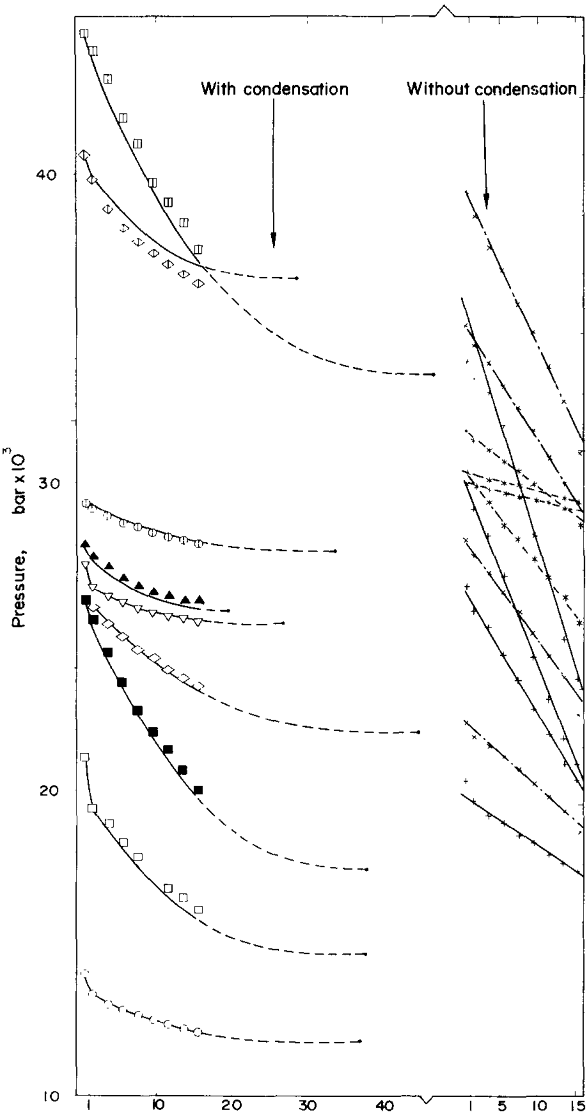

FIG. 9. Pressure distributions across tube banks. Symbols correspond to those in Table 2.

3.3 *Resistance coefficients*

Measurements of pressure drop of steam and their experimental conditions are shown in Fig. 9 and Table 2 respectively. While the pressure in non-condensing cases varies almost linearly, that in condensing cases varies non-linearly owing to the variation of mass velocity. To measure accurately the pressure drop over a tube bank, two pressure taps are usually set at a point upstream and at a point far enough downstream, where pressure is recovered. In these experiments, however, the pressure taps were set across the tube bank, and in order to prevent blockade by drain relatively large holes were inevitably used, and moreover, pressure itself fluctuated owing to the breathing flow aforementioned. Accordingly, it must be borne in mind that some unknown experimental errors are involved in the following discussion.

By applying the law of momentum to the steam flow in any control surface by i- and j-th cross section and neglecting the momentum of condensate, the following equation is derived,

$$p_i - p_j = c_D \frac{2(\zeta M_m)^2 \eta}{\bar{\rho}_m} - \left\{\left(\frac{\xi M^2}{\bar{\rho}}\right)_i - \left(\frac{\xi M^2}{\bar{\rho}}\right)_j\right\}. \tag{7}$$

In this equation it may be available that $\bar{\rho}_m = \bar{\rho}_i = \bar{\rho}_j =$ const. for a small number of tube rows in the control surfaces n, and that $\xi_i = \xi_j =$ const. for fully developed stream. In this paper ξ is taken as a unit, because it is not to be estimated correctly for the uncertain velocity distribution in the cross sections. The coefficient of flow resistance c_D will therefore be apparently under-estimated, though it will not exceed 20 per cent for this spacing-to-diameter ratio.

In non-condensing cases, since the variation of momentum is negligibly small, (7) is reduced to

$$p_i - p_j = c_D \frac{2(\zeta M^2) n}{\bar{\rho}_m}. \tag{8}$$

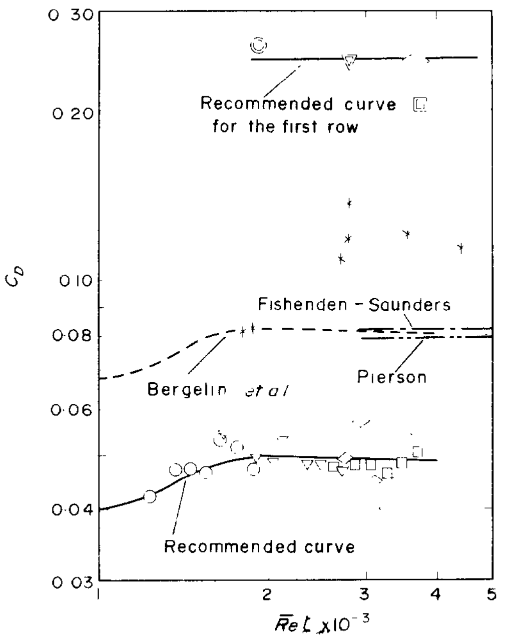

(a)

measurements at $(i, j) = (0,1), (1, 3), (3, 5), \ldots, (13, 15)$ successively into (7), and c_D in non-condensing cases by substituting the mean pressure gradient $(p_0 - p_{15})/15$ into equation (8). Thus evaluated c_D is shown in Fig. 10 as a function of $\overline{Re}_\zeta$, which is defined as

$$\overline{Re}_\zeta = \frac{\zeta M D}{\bar{\mu}}. \tag{9}$$

In the figure double symbols denote the values on the first tube row. In Fig. 10 are also inserted the curves obtained experimentally by Bergelin *et al.* [8], Kays *et al.* [9] and Pierson [10] and recommended by Fishenden and Saunders [11] in non-condensing cases. Each of them is selected as the example having similar spacing-to-diameter ratio to this apparatus.

The data shown in Fig. 10 scatter considerably on the whole, but allow the qualitative conclusions as follows; in condensing cases c_D for in-line arrangement is about a half of that for

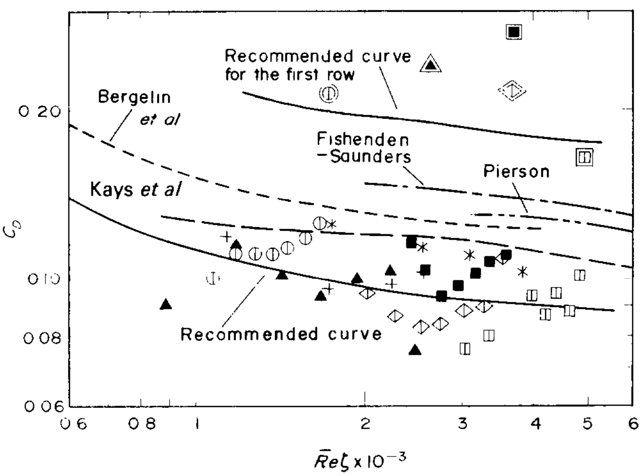

(b)

FIG. 10. Resistance coefficients. Symbols correspond to those in Table 2 and Fig. 9. (a) in-line, (b) staggered.

When i and j are taken as inlet and outlet of the tube bank respectively, this equation becomes the same as the usual definition of resistance coefficient.

The resistance coefficient c_D in condensing cases is evaluated by substituting pairs of the

staggered one, c_D for the first row is much larger than that for the successive ones, and c_D in condensing cases is smaller than that in non-condensing ones except for the first row.

It is well known about the boundary layer with suction that the frictional resistance increases and the drag decreases owing to the retardation of separation. For condensing steam through tube banks, the latter effect may be enlarged. In the experiments for in-line arrangement there was a whistle of about 1500–1600 cps, which was perhaps due to Kármán vortex, when steam did not condense, but it was arrested when steam began to condense. It may be appreciated from these facts that c_D was remarkably reduced owing to the change of the flow pattern of steam. Though the flow resistance with the first tube row is normally large, it is also apparently emphasized by substituting $\xi_1 = 1$ into (7).

In non-condensing cases the data on staggered arrangement are lower than any one of the reference curves, and are somewhat affected by the hole diameter of measuring taps. This disagreement is however the same order of the mutual differences of the reference curves. The data on in-line arrangement, on the other hand, are somewhat larger than the reference curves, which are scarcely different with each other.

Generally, resistance coefficient of flow through tube banks c_D depends remarkably on the relation between the diameter and the spacings of tubes. It is therefore convenient that c_D in condensing cases is given as the ratio to that in non-condensing cases, because the experimental data on the latter cases are available in the literature to a considerable extent. If the curves of Bergelin *et al.* are taken as the standard ones, for the time being, c_D in condensing cases is smaller than those about 40 and 25 per cent for in-line and staggered arrangement respectively. Especially c_D for the first row is about 5 and 2 times as large as the successive ones for in-line and staggered arrangement respectively. These recommended values are shown in Fig. 10 as solid curves.

3.4 *Pressure drops through tube banks*

We can calculate pressure drop through a tube bank by assuming that pressure p_0 and flow rate of steam M_0 at the inlet of the tube bank, and condensing rate G are given. Moreover, G may be appreciated to be constant commonly for all tube rows, because it is determined mainly by the temperature and velocity of cooling water.

Flow rate M_j and pressure p_j at jth cross section and necessary number of tube rows for complete condensation N are respectively,

$$M_j = M_0 - jG, \tag{10}$$

$$\begin{aligned} p_j - p_{j-1} &= \frac{1}{\bar{\rho}_{j-1}}\{2c_D\zeta^2 M_{j-1}^2 - (M_{j-1}^2 - M_j^2)\} \\ &= \frac{2M_0^2}{\bar{\rho}_{j-1}}\left\{c_D\zeta^2\left(1 - \frac{j-1}{N}\right)^2 \right. \\ &\qquad \left. - \frac{1}{N}\left(1 - \frac{j-\frac{1}{2}}{N}\right)\right\}, \end{aligned} \tag{11}$$

$$N = \frac{M_0}{G}, \tag{12}$$

where $j = 1, 2, \ldots, N$.

If c_D is given as a function of $\overline{Re}_\zeta$, pressure variation is obtained by successive calculation of (11). The curves inserted in Fig. 9 are obtained by assuming N with (12) and by substituting c_D recommended in Fig. 10 into (11). The calculated values and measurements are in good agreement in both trend and magnitude, except for the first row.

By assuming that both c_D and $\bar{\rho}$ do not vary, the following expressions are deduced from (11),

$$\begin{aligned} p_0 - p_j &= \frac{2c_D\zeta^2 M_0^2}{\bar{\rho}}\left\{j - \frac{j(j-1)}{N}\right. \\ &\quad \left. + \frac{j(j-1)(2j+1)}{6N^2}\right\} - \frac{2M_0^2}{\rho N}\left(j - \frac{j^2}{2N}\right), \end{aligned} \tag{13}$$

$$p_0 - p_N = \frac{M_0^2}{\bar{\rho}}\left\{\frac{c_D\zeta^2(N+1)(2N+1)}{3N} - 1\right\}. \tag{14}$$

For $c_D\zeta^2 N \gg 1$, these reduce to,

$$\frac{p_0 - p_j}{p_0 - p_N} = 3\frac{j}{N} - 3\left(\frac{j}{N}\right)^2 + \left(\frac{j}{N}\right)^3, \tag{15}$$

$$p_0 - p_N = \frac{2c_D\zeta^2 M_0^2 N}{3\bar{\rho}}. \tag{16}$$

These approximate expressions can be applicable to the part between first and Nth cross section.

The approximate values of $(p_1 - p_N)$ calculated by (14) and (16), where $\bar{\rho}$ and c_D at pressure p_1 and at pressure $(p_1 + p_2)/2$ corresponding to the $(1/5 \sim 1/4)$ Nth row are taken as the representative values respectively, are compared with the values of successive calculation in Table 3. The error in the column of p_1 vs. (16) for in-line arrangement is relatively small, because the errors owing to the choice of representative values and to the neglect of the term of momentum change cancel out mutually.

Figure 11 shows the pressure distributions nondimensionally. The results of successive calculations lie in the range between two solid lines for respective arrangements, and the experimental data are normalized by the results of each respective calculation $(p_1 - p_N)$. Chain lines represent the predictions by (15), which may be appreciated as practically good approximation.

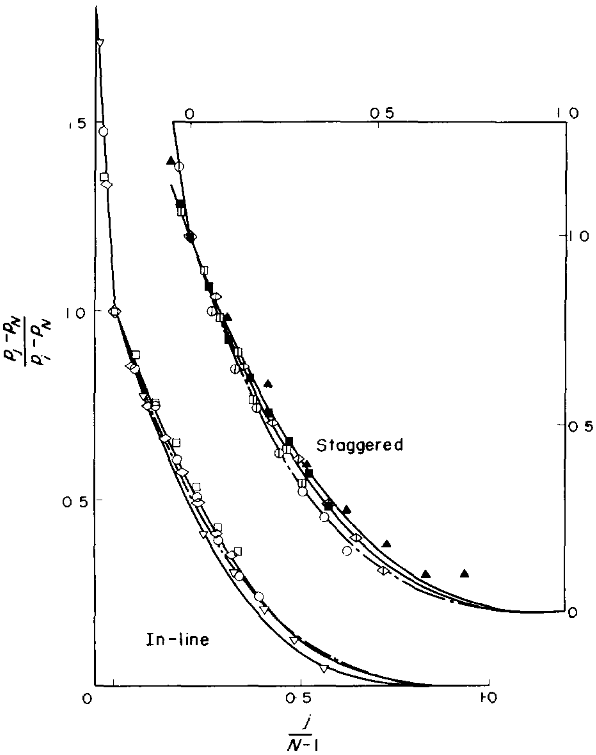

FIG. 11. Nondimensional pressure distributions across tube banks. Symbols correspond to those in Table 2 and Fig. 9.

Table 3. Accuracy of approximate expressions for pressure drop $(p_1 - p_N)$

	Reference pressure for $\bar{\rho}$, c_D	Error of (14) (%)	Error of (16) (%)
in-line	$(p_1 + p_N)/2$	$+2 \sim +5$	$+9 \sim +16$
	p_1	$-10 \sim +2$	$-3 \sim +10$
staggered	$(p_1 + p_N)/2$	$-4 \sim +1$	$-4 \sim +3$
	p_1	$-17 \sim -9$	$-15 \sim -6$

4. CONCLUSION

Condensation in horizontal cross flow of low pressure saturated steam through both in-line and staggered arranged tube banks of 14 mm dia. and 22 mm spacing, were studied experimentally. The following conclusions will be restricted rather to the aforementioned dimensions of tube banks, especially as to the resistance coefficients.

(1) Condensation process is not so simple as that treated in the previous theoretical researches even for filmwise. Effects of accumulation of leaked air are explained in Fig. 3 and temperature distributions on the tube surface are shown in Fig. 4.

(2) Heat-transfer coefficients of filmwise condensation are expressed nondimensionally by (6). Nusselt number for in-line arrangement is about 20 per cent lower than that for staggered arrangement. Heat transfer coefficients of dropwise condensation in forced flow of low pressure steam may be appreciated to be in the same order of those in quiescent steam. For low pressure steam, furthermore, heat-transfer coefficients of both modes of condensation are comparable to each other.

(3) Pressure distribution through tube banks can be calculated by (11) or (15), in which resistance coefficient c_D is recommended by

solid curves in Fig. 10. c_D for in-line arrangement is generally about a half of that for staggered one, and both of these are lower than those in non-condensing cases.

(4) Pressure drops over tube banks can be calculated by (14) or (16) with respective grade of approximation as shown in Table 3, but it must be calculated by (11) separately for only the first row.

ACKNOWLEDGEMENTS

The authors wish to express their appreciation to Manager Dr. Y. Takeda of Kawasaki Heavy Work Co. for his valuable suggestions. H. Fujishima, C. Kurata and Y. Hayamizu, who were senior students, and M. Wakamatsu, T. Tanoue, T. Kizuka and S. Tojo, who were graduate students, assisted with the experiment. M. Izumi assisted in the work of the manufacturing of the apparatus.

REFERENCES

1. T. Fujii, H. Uehara and C. Kurata, Laminar filmwise condensation of flowing vapour on a horizontal cylinder, *Int. J. Heat Mass Transfer* **15**, 235–246 (1972).
2. D. W. Tanner, D. Pope, C. J. Potter and D. West, Heat transfer in dropwise condensation at low steam pressure in the absence and presence of non-condensable gas, *Int. J. Heat Mass Transfer* **11**, 181–191 (1968).
3. A. R. Brown and M. A. Thomas, Filmwise and dropwise condensation of steam at low pressures, Proc. Third International Heat Transfer Conference, Chicago, vol. II, pp. 300–305 (1966).
4. L. D. Berman and U. A. Tumanov, Issledovanie teplootdachi pri kondensatsii dvijushtshegosa para na gorizontalinoi trube, *Teploenergetika* **10**, 77–83 (1962).
5. B. E. Short and H. E. Brown, Condensation of vapours on vertical banks of horizontal tubes, Proc. General Discussion on Heat Transfer, pp. 27–31 (1951).
6. F. L. Young and W. J. Wohlenberg, Condensation of saturated Freon-12 vapor on a bank of horizontal tubes, *Trans. Am. Soc. Mech. Engrs* **74**, 787–794 (1912).
7. V. A. Rachko, A study of the process of condensation of moving pure steam on arrays of tubes, *Sov. Phys. Tech. Phys.* **3**, 1151–1163 (1958).
8. O. P. Bergelin, G. A. Brown and S. C. Doberstein, Heat transfer and fluid friction during flow across banks of tubes—IV, *Trans. Am. Soc. Mech. Engrs* **74**, 953–960 (1952).
9. W. M. Kays, A. L. London and R. K. Lo, Heat-transfer and friction characteristics for gas flow normal to tube banks, *Trans. Am. Soc. Mech. Engrs* **76**, 387–396 (1954).
10. O. L. Pierson, Experimental investigation of the influence of tube arrangement on convection heat transfer and flow resistance in cross flow of gases over tube banks, *Trans. Am. Soc. Mech. Engrs* PRO-59-6, 563–572.
11. M. Fishenden and O. A. Saunders, *An Introduction to Heat Transfer*, p. 132. Clarendon Press, London (1950).

TRANSFERT THERMIQUE ET RÉSISTANCE AÉRODYNAMIQUE POUR UN ÉCOULEMENT DE VAPEUR EN CONDENSATION À BASSE PRESSION À TRAVERS UN FAISCEAU DE TUBES

Résumé—Cet article traite d'une expérience relative à la condensation lorsque une vapeur saturée à basse pression traverse horizontalement un faisceau de tubes. On propose des expressions simples pour les coefficients de transfert thermique du côté vapeur et la chute de pression à travers le réseau de tubes et on représente graphiquement les coefficients de résistance. On fait en même temps une comparaison entre les résultats relatifs à deux arrangements, l'un en ligne l'autre en quinconce, avec un rapport distance/diamètre égal à 22/14. On donne les résultats sur la distribution périphérique de température à la surface du tube, l'accumulation d'air éjecté, l'écoulement de la vapeur, etc......

WÄRMEÜBERGANG UND STRÖMUNGSWIDERSTAND BEI DER KONDENSATION VON NIEDERDRUCKDAMPF AN ROHRBÜNDELN

Zusammenfassung—Dieser Beitrag behandelt die Kondensation von gesättigtem Dampf bei niedrigem Druck an querangeströmten Rohrbündeln. Einfache Ausdrücke für Wärmeübergangskoeffizienten an der Dampfseite und für den Druckabfall im Rohrbündel werden vorgeschlagen. Widerstandsbeiwerte werden graphisch dargestellt. Gleichzeitig werden die Ergebnisse verglichen für Rohrbündel mit gerader und versetzter Rohranordnung, wobei das Verhältnis Abstand zu Rohrdurchmesser 22/14 ist. Ebenso werden die Beobachtungen über Temperaturverteilung an der Rohroberfläche, Ansammlung von Leckluft, Strömungsbewegung des Dampfes usw. erläutert.

ПЕРЕНОС ТЕПЛА И СОПРОТИВЛЕНИЕ ПОТОКУ ПРИ КОНДЕНСАЦИИ ПАРА НИЗКОГО ДАВЛЕНИЯ, ПРОХОДЯЩЕГО ЧЕРЕЗ ПУЧКИ ТРУБ

Аннотация—В статье описывается экспериментальное исследование конденсации, когда насыщенный пар низкого давления протекает через пучки труб, пересекая их в горизонтальном направлении. Предложены простые выражения для коэффициентов переноса тепла и падения давления через пучки труб. Коэффициенты сопротивления представлены графически. В то же время произведено сравнение результатов для двух пучков труб коридорного и махматного расположения при отношении шага к диаметру 22/14. Определены распределение температуры по поверхности труб, масса утекающего воздуха, циклически измсняющийся поток пара и т.д.